Title

The Memory of Environmental Chemical Exposure in C. elegans Is Dependent on the Jumonji Demethylases jmjd-2 and jmjd-3/utx-1

Journal

Cell Reports, 23(8)

ISSN

2639-1856

Authors

Camacho, Jessica

Truong, Lisa

Kurt, Zeyneb

et al.

Publication Date

2018-05-01

DOI

10.1016/j.celrep.2018.04.078

Peer reviewed

HHS Public Access

Author manuscript

Cell Rep. Author manuscript; available in PMC 2018 June 15.

Published in final edited form as:

Cell Rep. 2018 May 22; 23(8): 2392–2404. doi:10.1016/j.celrep.2018.04.078.

The Memory of Environmental Chemical Exposure in *C. elegans* Is Dependent on the Jumonji Demethylases *jmjd-2* and *jmjd-3/utx-1*

Jessica Camacho[1], **Lisa Truong**[2], **Zeyneb Kurt**[3], **Yen-Wei Chen**[1], **Marco Morselli**[4], **Gerardo Gutierrez**[1,5], **Matteo Pellegrini**[4], **Xia Yang**[1,3,6,7,8], and **Patrick Allard**[1,8,9,10,*]

[1]Molecular Toxicology Interdepartmental Program, University of California, Los Angeles, Los Angeles, CA 90095, USA

[2]Human Genetics and Genomic Analysis Training Program, University of California, Los Angeles, Los Angeles, CA 90095, USA

[3]Department of Integrative Biology and Physiology, University of California, Los Angeles, Los Angeles, CA 90095, USA

[4]Molecular, Cell and Developmental Biology Department, University of California, Los Angeles, Los Angeles, CA 90095, USA

[5]Department of Environmental and Occupational Health, California State University, Northridge, CA 91330, USA

[6]Bioinformatics Interdepartmental Program, University of California, Los Angeles, Los Angeles, CA 90095, USA

[7]Institute for Quantitative and Computational Biosciences, University of California, Los Angeles, Los Angeles, CA 90095, USA

[8]Molecular Biology Institute, University of California, Los Angeles, Los Angeles, CA 90095, USA

[9]Institute for Society and Genetics, University of California, Los Angeles, Los Angeles, CA 90095, USA

SUMMARY

*Correspondence: pallard@ucla.edu.

[10]Lead Contact

DATA AND SOFTWARE AVAILABILITY

The accession numbers for the ChIP-seq and RNA-seq data reported in this paper are GEO: GSE113187 and GSE113266.

SUPPLEMENTAL INFORMATION

Supplemental Information includes eight figures and five tables and can be found with this article online at https://doi.org/10.1016/j.celrep.2018.04.078.

AUTHOR CONTRIBUTIONS

J.C., L.T., M.M., and G.G. performed the experiments. J.C., L.T., Z.K., Y.-W.C., M.P., X.Y., and P.A. analyzed and interpreted the results. J.C., L.T., Z.K., Y.-W.C., X.Y., and P.A. wrote the manuscript.

DECLARATION OF INTERESTS

The authors declare no competing interests.

How artificial environmental cues are biologically integrated and transgenerationally inherited is still poorly understood. Here, we investigate the mechanisms of inheritance of reproductive outcomes elicited by the model environmental chemical Bisphenol A in *C. elegans*. We show that Bisphenol A (BPA) exposure causes the derepression of an epigenomically silenced transgene in the germline for 5 generations, regardless of ancestral response. Chromatin immunoprecipitation sequencing (ChIP-seq), histone modification quantitation, and immunofluorescence assays revealed that this effect is associated with a reduction of the repressive marks H3K9me3 and H3K27me3 in whole worms and in germline nuclei in the F3, as well as with reproductive dysfunctions, including germline apoptosis and embryonic lethality. Furthermore, targeting of the Jumonji demethylases JMJD-2 and JMJD-3/UTX-1 restores H3K9me3 and H3K27me3 levels, respectively, and it fully alleviates the BPA-induced transgenerational effects. Together, our results demonstrate the central role of repressive histone modifications in the inheritance of reproductive defects elicited by a common environmental chemical exposure.

In Brief

Little is known about the mechanisms of inheritance of artificial environmental exposures. Camacho et al. describe the transgenerational reproductive dysfunctions caused by ancestral exposure to the model environmental compound Bisphenol A, and they provide a role for the regulation of repressive histone marks by histone demethylases in this process.

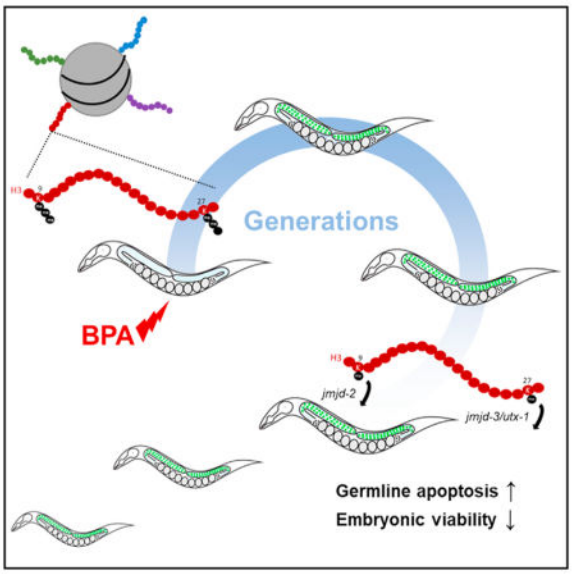

INTRODUCTION

The elicitation and inheritance of phenotypes from environmental cues have been the subject of intense research and debate. Best understood is the transfer of biological information triggered by natural exposures, such as temperature, hyperosmotic stress, diet, or starvation, thanks to research advances in a variety of model systems from plants to rodents (reviewed in Heard and Martienssen, 2014). Recent reports have shown that the heritability of effects elicited by such natural cues across generations is conditioned by changes in the epigenome,

or the molecular tags that alter gene expression and that are mitotically and/or meiotically heritable but do not entail a change in DNA sequence (Wu and Morris, 2001). These mechanisms include small RNA-based pathways (Gapp et al., 2014; Rechavi et al., 2014; Zhong et al., 2013) as well as through the regulation of the complex collection of covalent modifications of histone proteins (Gaydos et al., 2014; Greer et al., 2014; Kishimoto et al., 2017; Klosin et al., 2017; Siklenka et al., 2015). By contrast, the transgenerational inheritance of man-made environmental chemicals has remained controversial, particularly in mammalian settings. Several rodent studies have indicated that a one-generation parental (P)0 exposure to compounds, such as the fungicide Vinclozolin (Anway et al., 2005), or to mixtures of plastic compounds, such as Bisphenol A (BPA) and phthalates (Manikkam et al., 2013), is sufficient to cause a transgenerational decrease in the number and quality of germ cells in F3 and F4 adults, and it correlates with an alteration of DNA methylation patterns (Anway et al., 2005, 2006). However, some of these studies have been challenged (Heard and Martienssen, 2014; Hughes, 2014), have not provided a clear mechanism of inheritance, and have not explored the involvement of other epigenetic marks besides DNA methylation, such as histone modifications.

The nematode *Caenorhabditis elegans* has proven to be a valuable model system to study the effects of environmental exposures on the epigenome due to its ability to respond to a variety of stressors (Kishimoto et al., 2017; Klosin et al., 2017; Rechavi et al., 2014; Rudgalvyte et al., 2017). Here, we exploited the tractability of *C. elegans* to study the transgenerational impact of chemical exposure on reproductive function and dissect its underlying mechanisms of inheritance. These experiments were greatly facilitated by the nematode's short generation time, approximately 4 days at 20°C; its well-characterized distribution and regulation of chromatin marks (Bessler et al., 2010; Ho et al., 2014; Liu et al., 2011); and its ability to silence repetitive transgenes in the germline via repressive histone modifications in a fashion similar to the silencing of repetitive elements in mammalian germ cells (Kelly and Fire, 1998; Liu et al., 2014). Using these features, we investigated the mechanism of transgenerational inheritance following exposure to the model environmental chemical BPA. BPA is a widely used, high-production volume plastic manufacturing chemical highly prevalent in human samples (Vandenberg et al., 2010). We show that ancestral BPA exposure causes a histone 3, lysine 9 (H3K9) and a histone 3, lysine 27 (H3K27) trimethylation-dependent transgenerational chromatin-desilencing response in the germline that spans five generations and is associated with germline dysfunction and elevated progeny lethality.

RESULTS

Germline Transgene Desilencing following Chemical Exposure

To capture single, multi-, and transgenerational environmental effects stemming from chemical exposure, we used a germline desilencing reporter (Kelly et al., 1997). The assay that we developed (Figure 1A) is based on the strain NL2507 carrying an integrated low-complexity, highly repetitive array composed of a transgene coding for a fusion product between nuclear-localized LET-858 and GFP (*pkIs1582[let-858::GFP; rol-6(su1006)]*). This transgene is expressed in somatic cells, but it is transcriptionally silenced in the germline

(Figure 1B) via accumulation of the repressive marks H3K9me3 and H3K27me3 (Kelly and Fire, 1998; Schaner and Kelly, 2006).

We first tested the reporter NL2507 strain in a chemical assay by using a variety of well-characterized inhibitors of chromatin-modifying enzymes (Figure S1). All drug exposures were performed at the P0 generation for 48 hr, encompassing the window of L4 stage to day 1 of adulthood. Drug responses were compared to the vehicle DMSO in the context of which a low rate of desilencing is observed (14.3% ± 1.6%). Following treatment with all tested inhibitors of H3K9 or H3K27 demethylases, of non-selective methyltransferases or demethylases, as well as of histone acetyltransferases, the transgene expression remained silenced at levels comparable to the DMSO control. Conversely, HDAC inhibitors or methyltransferase inhibitors against either H3K9 or H3K27 all led to an increase in *pkIs1582* germline expression, with exposure to the class I HDAC inhibitor sodium butyrate and the SAM and EZH2 inhibitor 3-Deazaneplanocin A (DZnep) showing the highest levels of desilencing at P0, 32.5% ± 3.1% and 38.2% ± 1.9%, respectively ($p \leq 0.0001$ for both). Together, these results indicate that the desilencing of the *pkIs1582* array may serve as a sensitive and relevant indicator of chromatin mark-regulated transcriptional modulation.

BPA Exposure Causes a Heritable, Transgenerational Chromosomal Array-Desilencing Response

BPA was chosen as a test compound in the array-desilencing assay based on several lines of evidence that include changes in H3K27 histone methyltransferase Enhancer of Zeste homolog 2 (EZH2) expression (Bhan et al., 2014) and decreases in H3K9me3 levels in post-natal mouse oocytes (Trapphoff et al., 2013) and in H3K9 and H3K27 methylation levels in a variety of somatic cell types (Doherty et al., 2010; Singh and Li, 2012; Yeo et al., 2013).

First, we tested a range of BPA concentrations (10, 50, 100, and 500 μM), chosen based on previous dose-response analyses (Chen et al., 2016), to identify the lowest dose that led to a maximal desilencing effect. We initially performed the exposures at a single generation (P0) at L4 stage for 48 hr. We observed a dose-response relationship of the germline array de-silencing across generations, reaching saturation at 100 μM (45.0% ± 3.3% desilencing at the F3, $p \leq 0.001$) (Figure S2A). We also tested additional 48-hr exposure windows, including from L1 to L4 (Figure S2B) and from day 0 of adulthood (24 hr post-L4) to day 2 (Figure S2C). In all cases, we observed a significant desilencing of the germline array in the F3, although the generational kinetics varied between exposure windows and none reached the maximum F3 desilencing levels achieved by the L4-to-day 1 exposure window (Figure S2A). Thus, for all subsequent experiments, we exposed the worms to a single 100-μM BPA dose from L4 to day 1. This external dose is below previously characterized *C. elegans* doses measured by gas chromatography-mass spectrometry (GC-MS) to lead to an internal BPA concentration within human physiological range (Chen et al., 2016).

We then examined the rate of array desilencing over six generations following the single P0 generation BPA exposure at 100 μM (Figure 1C). The solvent control DMSO led to a pronounced elevation in desilencing in F1 animals (34.6% ± 5.4% of worms display GFP expression in their germline) compared to water alone (8.6% ± 0.8%). However, GFP levels in the DMSO group sharply declined after the F1 generation and were statistically

indistinguishable from the water control at the F4 generation. This effect of DMSO is likely due to its described positive activity in DNA relaxation, transcription enhancement, and promotion of an active chromatin state (Iwatani et al., 2006; Juang and Liu, 1987; Kim and Dean, 2004). By contrast, BPA exposure led to a dramatic increase in desilencing in the F1 generation (50.0% ± 3.5%). This BPA-induced desilencing rate was consistently higher than DMSO's and remained that way until the F5 generation. These results therefore indicate a potent transgenerational desilencing response stemming from BPA exposure and spanning 5 generations (P0–F4).

To determine whether most of the desilencing effect observed in the first transgenerational (F3) generation is primarily caused by descendants of strong P0 responders, we performed a series of lineage studies where individual P0 worms were segregated based on their germline GFP expression following BPA or DMSO exposure. Worms that showed germline desilencing at P0 following BPA exposure gave rise to F1, F2, and F3 progenies with a high rate of desilencing, nearing 60% (Figure 1D). By contrast, DMSO-exposed animals, whether silenced or desilenced at P0, showed a reduced rate of desilencing in the F2 and F3 generations, nearing 20%. Surprisingly, BPA-treated but GFP-negative P0 worms gave rise to progeny showing a higher rate of desilencing at each subsequent generation, such that there was a statistically significant difference when compared to DMSO in the F2 and F3 generations. In the latter, the proportion of descendants of BPA-exposed but GFP-negative P0s showing germline desilencing reached 42.3% ± 2.8% ($p \leq 0.01$ versus DMSO/GFP−). Interestingly, the mating of ancestrally exposed F1 hermaphrodites with unexposed males did not rescue the germline desilencing response, indicating that the primary mode of inheritance of BPA's effect is through the female germline (Figure S2D).

Collectively, these findings identify a matrilineal transgenerational inheritance of a repetitive array-desilencing response that is only partially conditioned by the ancestral (P0) response to BPA exposure.

BPA Exposure Causes a Transgenerational Alteration of the Germline Transcriptome

To investigate the impact of ancestral BPA exposure on the germline and distinguish it from that of DMSO, which also led to a mild transgenerational germline desilencing in the F3 compared to water, we performed RNA sequencing (RNA-seq) analysis on isolated F3 germlines. We identified a total of 264 transcripts that were differentially up- or downregulated at $p \leq 0.05$ in F3 germlines ancestrally exposed to BPA compared to DMSO, with 152 transcripts having a fold induction ≤0.5 or ≥1.5 (Table S1; Figure S3A). There was little overlap between the transcripts that were differentially expressed in all 3 groups, BPA versus DMSO, BPA versus water, and DMSO versus water (Figure S3B), suggesting that DMSO's transgenerational impact on the germline transcriptome is mostly distinct from that of BPA. A gene ontology analysis of the functional categories represented by the differentially expressed transcripts also highlighted the lack of overlap between the different treatment group comparisons. Interestingly, however, the second most represented functional category in the BPA versus DMSO group was reproduction, which was not represented in the DMSO versus water group (Figure S3C). This category includes 61 genes, many of them normally expressed in the germline tissue and essential for germline function (Table S2).

These results therefore suggest that ancestral BPA exposure may deregulate reproductive processes by altering the germline transcriptome.

Ancestral BPA Exposure Leads to a Deregulation of Repressive Histone Marks in F3 Nematodes

Several recent reports in *C. elegans* have implicated various histone modifications as important mediators of a variety of environmental effects across generations (Kishimoto et al., 2017; Klosin et al., 2017). We therefore assessed whether BPA exposure in P0 worms could lead to observable changes in the chromatin of F3 worms. To this aim, we performed chromatin immunoprecipitation sequencing (ChIP-seq) in whole adult worms at the F3 generation ancestrally exposed to BPA, DMSO, and water. Just as for the RNA-seq analysis, these experiments were performed on a large population of worms that were not selected based on their GFP expression. We focused our analysis on two repressive marks, H3K9me3 and H3K27me3, which have both been previously implicated in chromatin silencing in the germline of a wide range of species as well as in the repression of low-complexity transgenes in the *C. elegans* germline (Bessler et al., 2010; Greer et al., 2014; Leung et al., 2014; Liu et al., 2014; Schaner and Kelly, 2006; Towbin et al., 2012).

We first mined the ChIP-seq data to identify genes with significantly altered H3K9me3 and H3K27me3 levels (see the Experimental Procedures; Figures 2A and 2B). Among the three conditions, water, DMSO, and BPA, we identified between 3,740 and 4,951 broad peaks for H3K9me3 and between 19,019 and 21,741 for H3K27me3 (Table S3). A total of 1,055 and 1,780 genes were associated with broad peak calls, i.e., showed enrichment in their gene bodies, for H3K9me3 and H3K27me3, respectively. The majority of these peak calls were shared among all three treatment groups, although the BPA treatment group generated 88 and 59 unique peaks for H3K9me3 and H3K27me3, respectively (Figure 2B). The gene ontology (GO) analysis of biological processes at false discovery rate (FDR) < 0.05 and $p < 0.001$ for the genes associated with a loss of H3K27me3 broad peaks in BPA samples compared to DMSO confirmed the relevance of the epigenomic effect detected, as the second most prominent GO category was related to the response to steroid hormone stimulus, in line with BPA's well-described estrogenic activity (Table S4).

Next we compared the ChIP-seq and RNA-seq datasets by examining the levels of H3K9me3 and H3K27me3 under all 3 treatment conditions in genes that either had a low expression level in DMSO (first quartile, i.e., silenced genes) and were not upregulated or were upregulated >2-fold based on the RNA-seq data. As expected, we found that upregulated genes had on average 40%–50% lower H3K9me3 and H3K27me3 compared to their not-upregulated counterparts (Figures 2C and 2D). The levels and distributions of the marks were consistent with their described patterns in the *C. elegans* larval chromatin, where both H3K9me3 and H3K27me3 predominantly occupy the gene body of silenced genes (Ho et al., 2014). Comparing the three treatment groups, we did not observe a difference in H3K9me3 based on expression levels, perhaps due to the tissue sources used for the two datasets (whole worms for ChIP-seq and isolated germlines for RNA-seq). However, we observed a decrease in H3K27me3 in the BPA treatment group compared to DMSO and water for genes that were upregulated (Figure 2D, lightly shaded area indicates SE). These

results were similar for all genes, irrespective of expression level, where H3K27me3 was significantly reduced in the gene body compared to DMSO and water groups (Figure 3A).

Finally, we asked whether ancestral BPA exposure might not only affect H3K9me3 and H3K27me3 gene body levels but also their distribution along the chromosome axes. To this aim, we calculated the average fold enrichment of each mark over input by 1% increments along all 6 chromosomes. The data were normalized using a *Z* score for each individual chromosome and treatment group to allow the visualization of the marks' redistribution (Figure 3B). For each 1% increment, we also identified the number of peaks that were present in BPA but absent in DMSO (Figure 3C). These two complementary chromosome-wide analyses revealed a reduction of both marks from the distal chromosomal regions, largely heterochromatic (Garrigues et al., 2015), and a slight enrichment in the chromosome centers when comparing BPA to DMSO (Figures 3B and 3C). It also suggested a decrease of the marks' levels on the X chromosome. We validated the decrease in the levels of the marks by performing a multiplex histone post-translation modification (PTM) quantitation assay on pooled F3 whole-worm extracts (Table S5). The assay revealed a 25%–33% decrease in H3K9 mono-, di-, and trimethylation and a more pronounced 29%–56% decrease in H3K27 di- and trimethylation at the F3 generation in BPA-exposed P0 nematodes compared to DMSO. Conversely, another histone modification, H3K36me3, remained largely unchanged. Together, these results indicate a potent transgenerational impact of BPA on the chromatin, altering both the levels of the two repressive marks H3K9me3 and H3K27me3 as well as their distribution along chromosomal axes.

Ancestral BPA Exposure Leads to a Deregulation of Repressive Histone in the Germline

A transgenerational effect implies that the epigenomic alterations described above must also occur in the germline in order to be inherited. We therefore performed immunofluorescence against H3K9me3 and H3K27me3 in dissected germlines of the NL2507 strain containing the integrated *pkIs1582* transgene at the F3, when desilencing is pronounced, and at the F7, when germline desilencing has returned to control levels. At the pachytene stage of the F3 germline, we observed significant 26% and 24% reductions in global H3K9me3 and H3K27me3 levels, respectively, between BPA and DMSO (Figures 4A and 4B). By contrast, no significant differences were observed between water and DMSO. A similar decrease of total nuclear levels of these marks was seen in the strain PD7271, where the transgene is episomally maintained (*ccEx7271*): 23.3% and 34.6% reductions for H3K9me3 and H3K27me3, respectively (Figure S4). At the F7 generation, the germline levels of H3K9me3 and H3K27me3 in the BPA group were statistically indistinguishable from DMSO controls (Figure S5).

The use of the PD7271 *ccEx7271* array-bearing strain also allowed us to separately examine the levels of repressive modifications on the autosomes; the X chromosomes, which tend to lay apart from the rest of the chromosomes during the pachytene stage in hermaphrodites (Schaner and Kelly, 2006); and the extra-chromosomal array (Figures 5A and 5B). We observed marked decreases in both H3K9me3 and H3K27me3 on autosomes (24.8% and 34.3%, respectively), X chromosomes (25.3% and 41.5%), and the extrachromosomal array (39.6% and 51.3%). We examined whether the trend toward a larger decrease of these marks

on the X chromosomes compared to autosomes was significant by measuring the X:A ratio for each germline nucleus (Figure 5C). F3 germline nuclei showed a significant X:A ratio decrease in H3K27me3 levels when ancestrally exposed to BPA compared to DMSO (0.98 versus 1.09, respectively, a 10% decrease; $p = 0.03$), while H3K9me3 showed a trend toward a decreased X:A ratio between DMSO and BPA. Consistent with these results and with the described role of H3K27me3 in X silencing in the germline (Bender et al., 2006; Gaydos et al., 2012), we observed a modest but significant ($p = 0.01$) 2.36% increase in overall X-related genes with fragments per kilobase of transcript per million (FPKM) > 1 in our F3 germline RNA-seq data (Figure 5D).

Taken together, these experiments indicate a broad transgenerational impact on the germline chromatin of F3 nematodes not only confined to the repetitive arrays but also affecting the autosomes and the X chromosomes.

BPA Exposure Elicits a Transgenerational Increase in Embryonic Lethality and Germline Dysfunction

Next, we examined whether the transgenerational alteration of the germline chromatin was associated with reproductive defects. For these and all subsequent experiments, we chose to only compare BPA to DMSO, as BPA is dissolved in DMSO and the RNA-seq and ChIP-seq data indicated chromatin and expression BPA signatures distinct from those of DMSO. While the number of embryos produced was not dependent on ancestral exposure (Figure 6A), we observed a significant 85% ($D = 3.83$ and $B = 7.07$) increase in embryonic lethality in F3 worms ancestrally exposed to BPA when compared to DMSO (Figure 6B). We also examined the rate of embryonic lethality at the F7, a generation at which desilencing is not observed. Surprisingly, a trend between DMSO and BPA was still apparent even if it did not reach significance (86%, $D = 3.58$ and $B = 6.67$) (Figure 6B). The F3 embryonic lethality defect was not caused by the spurious expression of the *pkIs1582* transgene in the germline, as it was also observed in wild-type (N2) worms (Figure S6). Additionally, we assessed whether the increased embryonic lethality correlated with the transgene desilencing by separately assessing the embryonic survival of GFP-negative and GFP-positive F3 worms' progeny (Figure 6C). We observed a significantly higher level of embryonic lethality in the offspring of GFP-positive F3 worms ancestrally exposed to BPA when compared to both GFP-negative/BPA F3 offspring and GFP-positive/DMSO F3 offspring.

Finally, we monitored germline health by measuring the induction of germline apoptosis using acridine orange staining (Gartner et al., 2008) at the late prophase stage, when synapsis and recombination-dependent checkpoint activation results in programmed germline nuclear culling (Bhalla and Dernburg, 2005; Gartner et al., 2008). We observed a significant increase in germline apoptosis in F3 worms ancestrally exposed to BPA when compared to DMSO (Figures 6D and 6E), which was lost at the F7. Thus, together, these results show that ancestral BPA exposure elicits a clear transgenerational reproductive dysfunction effect. They also indicate that BPA-induced transgenerational effects mostly resolve by the F7.

Jumonji Histone Demethylase Activity Is Required for the Inheritance of BPA-Induced Transgenerational Effects

Since BPA exposure at the P0 generation was correlated with a decrease in repressive histone modifications in the germline of the F3 worms, we hypothesized that BPA's effects may be dependent on levels of these marks and on the activity of the enzymes that regulate them. This hypothesis was partially supported by the RNA-seq data from which 7 differentially expressed chromatin factors were identified: *sir-2.4*, ZK1127.3, *sop-2*, TO7E3.3, *met-2*, *jmjd-1.2*, and *set-26* (Table S1). MET-2, a SET domain histone H3 lysine 9 histone methyltransferase (HMTase) (Bessler et al., 2010), was significantly downregulated, while *set-26*, another H3K9 methyltransferase (Greer et al., 2014), was represented by two functionally equivalent transcript isoforms, one upregulated and one downregulated. Therefore, to functionally implicate the dysregulation of H3K9me3 and H3K27me3 in BPA's transgenerational outcomes, we attempted to rescue its effects by genetically or chemically modulating several histone demethylases after the initial P0 exposure but prior to the F3 (Figures 7A and S8A).

We first assessed whether the deregulation of repressive H3-lysine methylation marks by BPA is required for the transgenerational inheritance of BPA-induced effects. To this end, we used a feeding RNAi strategy to downregulate the expression of *jmjd-2* (H3K9me3/H3K36me3 histone lysine demethylase [KDM]) (Greer et al., 2014; Whetstine et al., 2006) or *jmjd-3/utx-1* (H3K27me3 KDM) (Agger et al., 2007), and we monitored two hallmarks of BPA's transgenerational effects, namely, the germline array desilencing as well as the increase in embryonic lethality. When compared to control RNAi, the downregulation of *jmjd-2* or *jmjd-3/utx-1* at the F1-to-F2 transition was sufficient to increase the levels of H3K9me3 and H3K27me3, respectively, in the F3 germlines (Figure 7B; quantification shown in Figure S7A). Also, while the control RNAi conditions slightly elevated the rates of desilencing and embryonic lethality compared to no-RNAi conditions, the downregulation of either *jmjd-2* or *jmjd-3/utx-1* led to a complete rescue of BPA-induced responses in the F3, except for the embryonic lethality effect under *jmjd-2* RNAi conditions, which was strongly reduced but did not reach significance (Figure 7C). Interestingly, single RNAi against *jmjd-3* or *utx-1* dramatically increased the proportion of desilenced germlines under both ancestral DMSO and BPA exposures, suggesting a partial compensation between *jmjd-3* and *utx-1* in the *C. elegans* germline (Figure S7B). This increase is similar to that of RNAi against the H3K27 HMT Polycomb Group complex member *mes-6* or against the SET domain H3K36 HMT *mes-4*, which functions to limit H3K27me3 spreading away from silenced chromatin (Figure S7B) (Gaydos et al., 2012).

We further implicated the deregulation of H3K9me3 and H3K27me3 as central to BPA's transgenerational effects by performing drug rescue experiments using the KDM4/JMJD-2 inhibitor IOX-1 (King et al., 2010), which has been shown to elevate H3K9me3 levels *in vitro* and in cell culture settings, (Hu et al., 2016; King et al., 2010; Schiller et al., 2014), and the potent selective Jumonji JMJD-3/UTX-1 H3K27 demethylase inhibitor GSK-J4 (Kruidenier et al., 2012). We first examined whether a combination of the two histone demethylase inhibitors would be sufficient to decrease the germline array desilencing and embryonic lethality effects. The co-treatment of the F1 generation with 100 μM IOX-1 and

100 μM GSK-J4 led to a significant reduction in BPA-induced array desilencing and embryonic lethality by 15.8% and 27.0%, respectively (Figure S8B). Finally, we tested the effect of the two inhibitors independently. Remarkably, F1 exposure to either IOX-1 or GSK-J4 was sufficient to suppress the elevation in array desilencing and embryonic lethality in P0 BPA-exposed worms compared to DMSO (Figure S8C). Thus, two distinct means of rescuing BPA's transgenerational effects, by RNAi or chemical inhibitors, indicate that the activity of either JMJD-2 or JMD-3/UTX-1 is required for the inheritance of BPA-induced reproductive effects.

DISCUSSION

In the present study, we aimed to characterize the molecular mechanisms of memory of environmental exposures using BPA as a model chemical. We showed that ancestral BPA exposure leads to a transgenerational decrease in the germline levels of H3K9me3 and H3K27me3 dependent on the activity of the JMJD-2 and JMJD-3/UTX-1 demethylases. Interestingly, our results indicate that, while the overt germline desilencing effect lasts only up to 5 generations, some modest impacts on reproduction extend at least until the F7 generation. These results therefore suggest that the transgenerational impact of BPA may differ depending on the type of genetic loci examined, with repetitive loci, such as the transgene, being less affected than other loci controlling *C. elegans* reproductive function.

We found that modulation of either JMJD-2 or JMJD-3/UTX-1 activity, chemically or genetically, is sufficient to dramatically reduce the inheritance of transgenerational effects. While JMJD-2 acts as both an H3K9me3 and H3K36me3 demethylase, the ability of *jmjd-2* RNAi to rescue desilencing's effects is likely caused by its action on H3K9me3, as H3K36me3 is considered an active mark in the *C. elegans* germline (Gaydos et al., 2012) and RNAi against *jmjd-2* increases its levels (Whetstine et al., 2006), which is inconsistent with the observed decrease in BPA-induced desilencing in *jmjd-2* RNAi F3 animals. Our results thus suggest a cooperation between H3K9me3 and H3K27me3 for proper chromatin silencing in the *C. elegans* germline. Such cooperation is understood in mammalian embryonic stem cells (ESCs) to emerge from the interaction between Jarid2/Jumonji and Polycomb Repressive Complex 2 (PRC2) (Pasini et al., 2010; Peng et al., 2009) and to be important for heterochromatin formation and/or maintenance through PRC2's effect on increasing the binding efficiency of HP1 to H3K9me3 (Boros et al., 2014). In *C. elegans*' embryonic or larval chromatin, there is a strong overlap between H3K27me3 and H3K9me3 at genome-wide levels (Garrigues et al., 2015; Ho et al., 2014). This overlap is particularly significant at chromosomal arms of heterochromatic nature as well as lamina-associated domains (Ho et al., 2014), something also observed in our data (Figure 3B). In the *C. elegans* meiotic germline, the overlap between H3K27me3 and H3K9me3 chromosomal distribution is likely to be high, as H3K27me3 distribution is greater than that of H3K9me3 (Bender et al., 2004; Bessler et al., 2010; Schaner and Kelly, 2006).

Our results are consistent with previous observations in mouse germ cells, where exposure of growing oocytes to low BPA concentrations decreased H3K9me3 levels (Trapphoff et al., 2013). However, the effect of BPA may also be context dependent, as an increase in EZH2 expression and, consequently, an elevation of H3K27me3 was detected in mammary tissues

following BPA exposure (Doherty et al., 2010). Our work suggests that, at least in *C. elegans*, the tight regulation of H3K9 and H3K27 methylation is central to the epigenetic memory of ancestral exposures. It will be crucial to examine how histone-based epimutations may be inherited across generations in mammalian models, since the mammalian epigenome undergoes two distinct waves of reprogramming, once in the primordial germ cells (PGCs) and a second time after fertilization in the pre-implantation embryo (reviewed in Tang et al., 2016). During the first reprogramming in PGCs, there is a wide fluctuation in H3K9me2 level, which becomes depleted (Seki et al., 2005), and in H3K27me3 level, which is gradually enriched globally (Hajkova et al., 2008). However, H3K9me3 is maintained in a dotted pattern in the pericentric heterochromatic regions as well as on endogenous retroviruses (Liu et al., 2014; Seki et al., 2005). Thus, H3K9me3 could serve in mammals as a molecular mediator of exposure memory in the germline.

The centrality of H3K9me3 in the inheritance of natural environmental effects has recently been further highlighted in *C. elegans*, where temperature-mediated alteration of transgene expression was detected for up to 14 generations (Klosin et al., 2017). However, other environmental cues, such as starvation or hyperosmosis, have been shown, depending on the studies, to require small RNA-based mechanisms and/or H3K4 trimethylase activity (Kishimoto et al., 2017; Rechavi et al., 2014). While these pathways may be mechanistically related, it will be necessary to examine whether a unifying mechanism of environmental inheritance can be identified, especially as we also identified a requirement for the regulation of H3K27 methylation for the transgenerational inheritance of BPA's exposure. Finally, our findings on the transgenerational memory of exposure to the model toxicant BPA and its impact on the germline's epigenome and reproduction also raise important questions for human risk from exposure, as our work identified transgenerational reproductive effects even in the absence of such a response in the earlier generations and at BPA concentrations lower than those previously characterized and that yielded internal concentrations close to those found in human reproductive tissues (Chen et al., 2016; Schönfelder et al., 2002; Vandenberg et al., 2010).

In conclusion, we have uncovered a transgenerational effect on reproduction stemming from exposure to the environmental chemical BPA and mediated in part by a deregulation of repressive histone modifications. These findings, therefore, highlight the need to comprehensively examine the effect of our chemical environment on the unique context of the germline epigenome, and they also offer interventional means to prevent the transmission of such effects across generations.

EXPERIMENTAL PROCEDURES

Culture Conditions and Strains

Standard methods of culturing and handling of *C. elegans* were followed (Stiernagle, 2006). Worms were maintained on nematode growth medium (NGM) plates streaked with OP50 *E. coli*, and all experiments were performed at 20°C (at 25°C, a pronounced desilencing of pkIs1582 is observed in the germ-line). Strains used in this study were obtained from the *C. elegans* Genetics Center (CGC) and include the following: NL2507 (*pkIs1582*[*let-858*::GFP; *rol-6*(*su1006*)]), PD7271 (*pha-1(e2123)* III*; ccEx7271*), and N2 (wild-type).

Chemical Exposure and GFP Scoring

The exposure and GFP germline desilencing assessments were performed as previously described (Lundby et al., 2016). Briefly, all chemicals tested were obtained from Sigma-Aldrich and were dissolved in DMSO to a stock concentration of 100 mM. Worms were synchronized by bleaching an adult population of the strain of interest, plating the eggs, and allowing the synchronized population to reach L4 larval stage (approximately 50 hr). These were then collected and incubated for 48 hr in 50 μL OP50 bacteria, 500 μL M9, and 0.5 μL of the chemical of interest for a final chemical concentration of 100 μM. After 48 hr, the worms were collected and allowed to recover on NGM plates for 1–2 hr (mixed population) or immediately plated as individual worms to separately labeled 35-mm seeded NGM plates (GFP+/− population sorting) and recovered there. Worms were scored for germline GFP expression using a Nikon H600L microscope at 40× magnification.

Apoptosis Assay and Embryonic Lethality Assessment

Apoptosis assay was performed by acridine orange staining on synchronized adult hermaphrodites collected at 20–24 hr post-L4, as previously described (Allard and Colaiácovo, 2011; Chen et al., 2016). Embryonic lethality was performed by monitoring the numbers of embryos produced by each worm of each day of its reproductive life and subsequent larvae hatched from these embryos. The ratio of the latter measure by the former and multiplied by 100 generates the rate of embryonic lethality.

Chemical Rescue

F1 L4 larvae were obtained from DMSO- or BPA-exposed GFP-positive P0 worm populations, and they were exposed for 48 hr to the chemical rescue drugs IOX-1 and GSK-J4 dissolved in DMSO to a stock concentration of 100 mM. In combination treatments, one drug was prepared at a higher concentration so that the final DMSO concentration never exceeded 0.11%. The exposed F1 adult worms were then allowed to recover on NGM plates, and their offspring were followed until the F3 generation for GFP scoring and embryonic lethality assessment.

RNAi Experiments

Worms were exposed to RNAi by feeding (Kamath and Ahringer, 2003) with *E. coli* strains containing either an empty control vector (L4440) or expressing double-stranded RNA. RNAi constructs against *jmjd-2*, *jmjd-3*, *utx-1*, *mes-4*, and *mes-6* were obtained from the Ahringer RNAi library and sequence verified. P0 worms were exposed to BPA or DMSO for 48 hr following the procedure described above. For *jmjd-2* and *jmjd-3*/*utx-1* RNAi, F1 adult worms from GFP-positive P0 worms were placed on plates of *E. coli* containing an empty control vector (L4440) or expressing double-stranded RNA to lay overnight. F2 worms were grown on RNAi bacteria from hatching until the first day of adulthood, at which point they were transferred to non-RNAi OP50 plates. The subsequent generation (F3) was collected at adulthood (24 hr post-L4) for further analysis. For *mes-4* and *mes-6* RNAi, the same procedure was followed but from the F2 to F3 generation to circumvent their associated maternal sterility phenotype.

Immunofluorescence

Immunofluorescence images were collected at 0.5-μm z intervals with an Eclipse Ni-E microscope (Nikon) and a cooled charge-coupled device (CCD) camera (model CoolSNAP HQ, Photometrics) controlled by the NIS Elements AR system (Nikon). The images presented and quantified are projections approximately halfway through 3D data stacks of *C. elegans* gonads, which encompass entire nuclei. Images were subjected to 3D landweber deconvolution analysis (5 iterations) with the NIS Elements AR analysis program (Nikon). H3K27me3 and H3K9me3 quantification in mid-late pachytene germ cell nuclei was performed with the ImageJ software. F3 worms were staged at L4, and gonad dissection and immunofluorescence were performed 20–24 hr post-L4, as previously described (Chen et al., 2016). Primary antibodies were used at the following dilutions: rabbit α-H3K9me3, 1:500 (Abcam); and mouse α-H3K27me2me3, 1:200 (Active Motif). Secondary antibodies were used at the following dilutions: Cy3 α-rabbit, 1:700; and TxRed α-mouse, 1:200, (Jackson ImmunoResearch).

Germline RNA Amplification and RNA-Seq Analysis

Total RNA was extracted from needle-dissected gonads of F3 adult worms obtained from a mixed population of H_2O-, DMSO-, and BPA-exposed P0 nematodes. The experiments were performed on 4 biological replicates of 30 gonads each that were processed through the NucleoSpin RNA XS, Macherey Nagel kit. cDNA was synthesized using the SMART-Seq v4 Ultra Low Input RNA Kit for sequencing, amplified 10×, and purified using agentcourt AMPure beads.

Nextera XT Library Prep Kit was used to prepare the sequencing libraries from 1 ng cDNA. Single-end sequencing at 50-bp length was performed on an Illumina Hiseq 4000 system (Illumina, CA, USA), and a total of ~350 million reads was obtained for 12 samples (3 treatment groups × 4 replicates/group). Data quality checks were performed using the FastQC tool (http://www.bioinformatics.babraham.ac.uk/projects/fastqc). RNA-seq reads passing quality control (QC) were analyzed using a pipeline comprised of HISAT (Kim et al., 2015), StringTie (Pertea et al., 2015), and Ballgown (Frazee et al., 2015) tools. HISAT was used to align reads against the *C. elegans* genome to discover the locations from which the reads originated and to determine the transcript splice sites. Then, StringTie was used to assemble the RNA-seq alignments into potential transcripts. Ballgown was used to identify the transcripts and genes that were differentially expressed between the BPA and DMSO groups, between the BPA and control (water) groups, and between the DMSO and control groups. FPKMs for each transcript were obtained by Ballgown and used as the expression measure. We filtered out the low-abundance transcripts and kept those having a mean FPKM > 1 across all samples. To test the transcriptional impact of BPA on individual chromosomes, we applied a Student's t test to determine whether the differences in the mean log2(FPKM + 1) values between the BPA and DMSO groups were significant for all transcripts with FPKM > 1 on each chromosome. $p \leq 0.05$ was considered significant.

ChIP-Seq and Multiplex PTM Assay

Histone modification H3K9me3 and H3K27me3 ChIP-seq data were generated as a service by Active Motif using their in-house antibodies from 3 biological repeats of frozen F3

nematode populations, with 200 μL worms per sample repeat. The sequencing data were obtained through Illumina Nextseq and mapped to ce10 genome by Burrows-Wheeler Aligner (BWA) algorithm (Li and Durbin, 2009). Following pooling of the sequencing data per exposure category (Yang et al., 2014), the data were normalized to input and million reads to produce a signal track file by MACS2 (Zhang et al., 2008). For chromosome-wide mark distribution analysis, each chromosome was divided into 100 sub-regions and average fold enrichment score per base in sub-regions. We normalized signals with Z score for each chromosome and each sample.

For gene body histone modification analysis, deepTools (Ramírez et al., 2014) was utilized to obtain aggregated signal from −500 bp of the upstream transcription start site (TSS) to +500 bp of the downstream transcription end site (TES). We first summarized genes with multiple transcripts into a single gene by the one with the most significant difference from BPA and DMSO from RNA-seq results. Silenced genes were defined as genes expressed in the lowest 25% (Q1, 1,801 genes) of all genes in the DMSO group, and upregulated genes were defined as silenced genes upregulated more than 2-fold after BPA treatment (244 genes) based on RNA-seq results. We called peaks by MACS2 broad peak function with q value = 0.1 (cutoff). Broad peak is used as a peak-calling category when analyzing data for protein-DNA association with broader DNA coverage, such as for H3K9me3 and H3K27me3. It joins nearby narrower peak calling into one broader peak. To compare differential peak, unique peak method was used to compare BPA and DMSO samples (Steinhauser et al., 2016). Non-overlapping broad peaks called by MACS2 were defined as unique peaks. Unique peaks from BPA and DMSO in 100 sub-regions along each chromosome were compared. We further define peaked genes as genes with any peak calling in gene body region. Unless specified, analyses were conducted by R 3.4.0 (R Core Team, 2017) and Bio-conductor (Huber et al., 2015).

The multiplex PTM quantitation assay was also generated as service by Active Motif on a Luminex platform, and it was performed on pooled samples (totaling 100 μL) generated from 3–4 individual repeats per exposure condition.

Statistical Analyses

Unless indicated otherwise, an unpaired t test assuming unequal variance with Welch’s correction was applied. For multi-group comparisons, a one-way ANOVA with Sidak correction or two-way ANOVA was used.

Supplementary Material

Refer to Web version on PubMed Central for supplementary material.

Acknowledgments

P.A. is supported by NIH/NIEHS R01 ES02748701 and the Burroughs Well-come Foundation. J.C. received support from NIH/NIEHS T32 ES015457 Training in Molecular Toxicology, the North American Graduate Fellowship, the NSF AGEP Competitive Edge, the NSF Graduate Research Fellowship, and the Eugene-Cota Robles Fellowship. L.T. is supported by the NIH Training Grant in Genomic Analysis and Interpretation T32 HG002536. G.G. is supported by NIH/NIEHS R25 ES02550703. Z.K. was supported by an American Heart Association post-doctoral fellowship (17POST33670739) and the Iris Cantor-UCLA Executive Advisory Board/

CTSI Pilot Award. M.M. was supported by a Dissertation Year Fellowship (University of California, Los Angeles). X.Y. is supported by NIH/NIDDK R01 DK104363 and NIH/NINDS R21 NS103088.

References

Agger K, Cloos PA, Christensen J, Pasini D, Rose S, Rappsilber J, Issaeva I, Canaani E, Salcini AE, Helin K. UTX and JMJD3 are histone H3K27 demethylases involved in HOX gene regulation and development. Nature. 2007; 449:731–734. [PubMed: 17713478]

Allard P, Colaiácovo MP. Mechanistic insights into the action of Bisphenol A on the germline using C. elegans. Cell Cycle. 2011; 10:183–184. [PubMed: 21228622]

Anway MD, Cupp AS, Uzumcu M, Skinner MK. Epigenetic transgenerational actions of endocrine disruptors and male fertility. Science. 2005; 308:1466–1469. [PubMed: 15933200]

Anway MD, Leathers C, Skinner MK. Endocrine disruptor vinclozolin induced epigenetic transgenerational adult-onset disease. Endocrinology. 2006; 147:5515–5523. [PubMed: 16973726]

Bender LB, Cao R, Zhang Y, Strome S. The MES-2/MES-3/MES-6 complex and regulation of histone H3 methylation in C. elegans. Curr Biol. 2004; 14:1639–1643. [PubMed: 15380065]

Bender LB, Suh J, Carroll CR, Fong Y, Fingerman IM, Briggs SD, Cao R, Zhang Y, Reinke V, Strome S. MES-4: an auto-some-associated histone methyltransferase that participates in silencing the X chromosomes in the C. elegans germ line. Development. 2006; 133:3907–3917. [PubMed: 16968818]

Bessler JB, Andersen EC, Villeneuve AM. Differential localization and independent acquisition of the H3K9me2 and H3K9me3 chromatin modifications in the Caenorhabditis elegans adult germ line. PLoS Genet. 2010; 6:e1000830. [PubMed: 20107519]

Bhalla N, Dernburg AF. A conserved checkpoint monitors meiotic chromosome synapsis in Caenorhabditis elegans. Science. 2005; 310:1683–1686. [PubMed: 16339446]

Bhan A, Hussain I, Ansari KI, Bobzean SA, Perrotti LI, Mandal SS. Histone methyltransferase EZH2 is transcriptionally induced by estradiol as well as estrogenic endocrine disruptors bisphenol-A and diethylstilbestrol. J Mol Biol. 2014; 426:3426–3441. [PubMed: 25088689]

Boros J, Arnoult N, Stroobant V, Collet JF, Decottignies A. Polycomb repressive complex 2 and H3K27me3 cooperate with H3K9 methylation to maintain heterochromatin protein 1α at chromatin. Mol Cell Biol. 2014; 34:3662–3674. [PubMed: 25047840]

Chen Y, Shu L, Qiu Z, Lee DY, Settle SJ, Que Hee S, Telesca D, Yang X, Allard P. Exposure to the BPA-Substitute Bisphenol S Causes Unique Alterations of Germline Function. PLoS Genet. 2016; 12:e1006223. [PubMed: 27472198]

Doherty LF, Bromer JG, Zhou Y, Aldad TS, Taylor HS. In utero exposure to diethylstilbestrol (DES) or bisphenol-A (BPA) increases EZH2 expression in the mammary gland: an epigenetic mechanism linking endocrine disruptors to breast cancer. Horm Cancer. 2010; 1:146–155. [PubMed: 21761357]

Frazee AC, Pertea G, Jaffe AE, Langmead B, Salzberg SL, Leek JT. Ballgown bridges the gap between transcriptome assembly and expression analysis. Nat Biotechnol. 2015; 33:243–246. [PubMed: 25748911]

Gapp K, Jawaid A, Sarkies P, Bohacek J, Pelczar P, Prados J, Farinelli L, Miska E, Mansuy IM. Implication of sperm RNAs in transgenerational inheritance of the effects of early trauma in mice. Nat Neurosci. 2014; 17:667–669. [PubMed: 24728267]

Garrigues JM, Sidoli S, Garcia BA, Strome S. Defining heterochromatin in C. elegans through genome-wide analysis of the heterochromatin protein 1 homolog HPL-2. Genome Res. 2015; 25:76–88. [PubMed: 25467431]

Gartner A, Boag PR, Blackwell TK. Germline survival and apoptosis. WormBook. 2008:1–20.

Gaydos LJ, Rechtsteiner A, Egelhofer TA, Carroll CR, Strome S. Antagonism between MES-4 and Polycomb repressive complex 2 promotes appropriate gene expression in C. elegans germ cells. Cell Rep. 2012; 2:1169–1177. [PubMed: 23103171]

Gaydos LJ, Wang W, Strome S. Gene repression. H3K27me and PRC2 transmit a memory of repression across generations and during development. Science. 2014; 345:1515–1518. [PubMed: 25237104]

Greer EL, Beese-Sims SE, Brookes E, Spadafora R, Zhu Y, Rothbart SB, Aristizábal-Corrales D, Chen S, Badeaux AI, Jin Q, et al. A histone methylation network regulates transgenerational epigenetic memory in C. elegans. Cell Rep. 2014; 7:113–126. [PubMed: 24685137]

Hajkova P, Ancelin K, Waldmann T, Lacoste N, Lange UC, Cesari F, Lee C, Almouzni G, Schneider R, Surani MA. Chromatin dynamics during epigenetic reprogramming in the mouse germ line. Nature. 2008; 452:877–881. [PubMed: 18354397]

Heard E, Martienssen RA. Transgenerational epigenetic inheritance: myths and mechanisms. Cell. 2014; 157:95–109. [PubMed: 24679529]

Ho JW, Jung YL, Liu T, Alver BH, Lee S, Ikegami K, Sohn KA, Minoda A, Tolstorukov MY, Appert A, et al. Comparative analysis of metazoan chromatin organization. Nature. 2014; 512:449–452. [PubMed: 25164756]

Hu Q, Chen J, Zhang J, Xu C, Yang S, Jiang H. IOX1, a JMJD2A inhibitor, suppresses the proliferation and migration of vascular smooth muscle cells induced by angiotensin II by regulating the expression of cell cycle-related proteins. Int J Mol Med. 2016; 37:189–196. [PubMed: 26530537]

Huber W, Carey VJ, Gentleman R, Anders S, Carlson M, Carvalho BS, Bravo HC, Davis S, Gatto L, Girke T, et al. Orchestrating high-throughput genomic analysis with Bioconductor. Nat Methods. 2015; 12:115–121. [PubMed: 25633503]

Hughes V. Epigenetics: The sins of the father. Nature. 2014; 507:22–24. [PubMed: 24598623]

Iwatani M, Ikegami K, Kremenska Y, Hattori N, Tanaka S, Yagi S, Shiota K. Dimethyl sulfoxide has an impact on epigenetic profile in mouse embryoid body. Stem Cells. 2006; 24:2549–2556. [PubMed: 16840553]

Juang JK, Liu HJ. The effect of DMSO on natural DNA conformation in enhancing transcription. Biochem Biophys Res Commun. 1987; 146:1458–1464. [PubMed: 3040003]

Kamath RS, Ahringer J. Genome-wide RNAi screening in Caenorhabditis elegans. Methods. 2003; 30:313–321. [PubMed: 12828945]

Kelly WG, Fire A. Chromatin silencing and the maintenance of a functional germline in Caenorhabditis elegans. Development. 1998; 125:2451–2456. [PubMed: 9609828]

Kelly WG, Xu S, Montgomery MK, Fire A. Distinct requirements for somatic and germline expression of a generally expressed Caernorhabditis elegans gene. Genetics. 1997; 146:227–238. [PubMed: 9136012]

Kim A, Dean A. Developmental stage differences in chromatin subdomains of the beta-globin locus. Proc Natl Acad Sci USA. 2004; 101:7028–7033. [PubMed: 15105444]

Kim D, Langmead B, Salzberg SL. HISAT: a fast spliced aligner with low memory requirements. Nat Methods. 2015; 12:357–360. [PubMed: 25751142]

King ON, Li XS, Sakurai M, Kawamura A, Rose NR, Ng SS, Quinn AM, Rai G, Mott BT, Beswick P, et al. Quantitative high-throughput screening identifies 8-hydroxyquinolines as cell-active histone demethylase inhibitors. PLoS ONE. 2010; 5:e15535. [PubMed: 21124847]

Kishimoto S, Uno M, Okabe E, Nono M, Nishida E. Environmental stresses induce transgenerationally inheritable survival advantages via germline-to-soma communication in Caenorhabditis elegans. Nat Commun. 2017; 8:14031. [PubMed: 28067237]

Klosin A, Casas E, Hidalgo-Carcedo C, Vavouri T, Lehner B. Transgenerational transmission of environmental information in *C. elegans*. Science. 2017; 356:320–323. [PubMed: 28428426]

Kruidenier L, Chung CW, Cheng Z, Liddle J, Che K, Joberty G, Bantscheff M, Bountra C, Bridges A, Diallo H, et al. A selective jumonji H3K27 demethylase inhibitor modulates the proinflammatory macrophage response. Nature. 2012; 488:404–408. [PubMed: 22842901]

Leung D, Du T, Wagner U, Xie W, Lee AY, Goyal P, Li Y, Szulwach KE, Jin P, Lorincz MC, Ren B. Regulation of DNA methylation turnover at LTR retrotransposons and imprinted loci by the histone methyl-transferase Setdb1. Proc Natl Acad Sci USA. 2014; 111:6690–6695. [PubMed: 24757056]

Li H, Durbin R. Fast and accurate short read alignment with Burrows-Wheeler transform. Bioinformatics. 2009; 25:1754–1760. [PubMed: 19451168]

Liu T, Rechtsteiner A, Egelhofer TA, Vielle A, Latorre I, Cheung MS, Ercan S, Ikegami K, Jensen M, Kolasinska-Zwierz P, et al. Broad chromosomal domains of histone modification patterns in C. elegans. Genome Res. 2011; 21:227–236. [PubMed: 21177964]

Liu S, Brind'Amour J, Karimi MM, Shirane K, Bogutz A, Lefebvre L, Sasaki H, Shinkai Y, Lorincz MC. Setdb1 is required for germline development and silencing of H3K9me3-marked endogenous retroviruses in primordial germ cells. Genes Dev. 2014; 28:2041–2055. [PubMed: 25228647]

Lundby Z, Camacho J, Allard P. Fast Functional Germline and Epigenetic Assays in the Nematode Caenorhabditis elegans. Methods Mol Biol. 2016; 1473:99–107. [PubMed: 27518628]

Manikkam M, Tracey R, Guerrero-Bosagna C, Skinner MK. Plastics derived endocrine disruptors (BPA, DEHP and DBP) induce epigenetic transgenerational inheritance of obesity, reproductive disease and sperm epi-mutations. PLoS ONE. 2013; 8:e55387. [PubMed: 23359474]

Pasini D, Cloos PA, Walfridsson J, Olsson L, Bukowski JP, Johansen JV, Bak M, Tommerup N, Rappsilber J, Helin K. JARID2 regulates binding of the Polycomb repressive complex 2 to target genes in ES cells. Nature. 2010; 464:306–310. [PubMed: 20075857]

Peng JC, Valouev A, Swigut T, Zhang J, Zhao Y, Sidow A, Wysocka J. Jarid2/Jumonji coordinates control of PRC2 enzymatic activity and target gene occupancy in pluripotent cells. Cell. 2009; 139:1290–1302. [PubMed: 20064375]

Pertea M, Pertea GM, Antonescu CM, Chang TC, Mendell JT, Salzberg SL. StringTie enables improved reconstruction of a transcriptome from RNA-seq reads. Nat Biotechnol. 2015; 33:290–295. [PubMed: 25690850]

R Core Team. R: A language and environment for statistical computing. R Foundation for Statistical Computing; 2017.

Ramírez F, Dündar F, Diehl S, Grüning BA, Manke T. deepTools: a flexible platform for exploring deep-sequencing data. Nucleic Acids Res. 2014; 42:W187–W191. [PubMed: 24799436]

Rechavi O, Houri-Ze'evi L, Anava S, Goh WSS, Kerk SY, Hannon GJ, Hobert O. Starvation-induced transgenerational inheritance of small RNAs in C. elegans. Cell. 2014; 158:277–287. [PubMed: 25018105]

Rudgalvyte M, Peltonen J, Lakso M, Wong G. Chronic MeHg exposure modifies the histone H3K4me3 epigenetic landscape in Caenorhabditis elegans. Comp Biochem Physiol C Toxicol Pharmacol. 2017; 191:109–116. [PubMed: 27717699]

Schaner CE, Kelly WG. Germline chromatin. WormBook. 2006:1–14.

Schiller R, Scozzafava G, Tumber A, Wickens JR, Bush JT, Rai G, Lejeune C, Choi H, Yeh TL, Chan MC, et al. A cell-permeable ester derivative of the JmjC histone demethylase inhibitor IOX1. Chem Med Chem. 2014; 9:566–571. [PubMed: 24504543]

Schönfelder G, Wittfoht W, Hopp H, Talsness CE, Paul M, Chahoud I. Parent bisphenol A accumulation in the human maternal-fetal-placental unit. Environ Health Perspect. 2002; 110:A703–A707. [PubMed: 12417499]

Seki Y, Hayashi K, Itoh K, Mizugaki M, Saitou M, Matsui Y. Extensive and orderly reprogramming of genome-wide chromatin modifications associated with specification and early development of germ cells in mice. Dev Biol. 2005; 278:440–458. [PubMed: 15680362]

Siklenka K, Erkek S, Godmann M, Lambrot R, McGraw S, Lafleur C, Cohen T, Xia J, Suderman M, Hallett M, et al. Disruption of histone methylation in developing sperm impairs offspring health transgenerationally. Science. 2015; 350:aab2006. [PubMed: 26449473]

Singh S, Li SS. Epigenetic effects of environmental chemicals bisphenol A and phthalates. Int J Mol Sci. 2012; 13:10143–10153. [PubMed: 22949852]

Steinhauser S, Kurzawa N, Eils R, Herrmann C. A comprehensive comparison of tools for differential ChIP-seq analysis. Brief Bioinform. 2016; 17:953–966. [PubMed: 26764273]

Stiernagle T. Maintenance of C. elegans. WormBook. 2006:1–11.

Tang WW, Kobayashi T, Irie N, Dietmann S, Surani MA. Specification and epigenetic programming of the human germ line. Nat Rev Genet. 2016; 17:585–600. [PubMed: 27573372]

Towbin BD, González-Aguilera C, Sack R, Gaidatzis D, Kalck V, Meister P, Askjaer P, Gasser SM. Step-wise methylation of histone H3K9 positions heterochromatin at the nuclear periphery. Cell. 2012; 150:934–947. [PubMed: 22939621]

Trapphoff T, Heiligentag M, El Hajj N, Haaf T, Eichenlaub-Ritter U. Chronic exposure to a low concentration of bisphenol A during follicle culture affects the epigenetic status of germinal vesicles and metaphase II oocytes. Fertil Steril. 2013; 100:1758–1767.e1. [PubMed: 24034936]

Vandenberg LN, Chahoud I, Heindel JJ, Padmanabhan V, Paumgartten FJR, Schoenfelder G. Urinary, circulating, and tissue bio-monitoring studies indicate widespread exposure to bisphenol A. Environ Health Perspect. 2010; 118:1055–1070. [PubMed: 20338858]

Whetstine JR, Nottke A, Lan F, Huarte M, Smolikov S, Chen Z, Spooner E, Li E, Zhang G, Colaiacovo M, Shi Y. Reversal of histone lysine trimethylation by the JMJD2 family of histone demethylases. Cell. 2006; 125:467–481. [PubMed: 16603238]

Wu CT, Morris JR. Genes, genetics, and epigenetics: a correspondence. Science. 2001; 293:1103–1105. [PubMed: 11498582]

Yang Y, Fear J, Hu J, Haecker I, Zhou L, Renne R, Bloom D, McIntyre LM. Leveraging biological replicates to improve analysis in ChIP-seq experiments. Comput Struct Biotechnol J. 2014; 9:e201401002. [PubMed: 24688750]

Yeo M, Berglund K, Hanna M, Guo JU, Kittur J, Torres MD, Abramowitz J, Busciglio J, Gao Y, Birnbaumer L, Liedtke WB. Bisphenol A delays the perinatal chloride shift in cortical neurons by epigenetic effects on the Kcc2 promoter. Proc Natl Acad Sci USA. 2013; 110:4315–4320. [PubMed: 23440186]

Zhang Y, Liu T, Meyer CA, Eeckhoute J, Johnson DS, Bernstein BE, Nusbaum C, Myers RM, Brown M, Li W, Liu XS. Model-based analysis of ChIP-Seq (MACS). Genome Biol. 2008; 9:R137. [PubMed: 18798982]

Zhong SH, Liu JZ, Jin H, Lin L, Li Q, Chen Y, Yuan YX, Wang ZY, Huang H, Qi YJ, et al. Warm temperatures induce transgenerational epigenetic release of RNA silencing by inhibiting siRNA biogenesis in Arabidopsis. Proc Natl Acad Sci USA. 2013; 110:9171–9176. [PubMed: 23686579]

Highlights

- Bisphenol A elicits a 5-generation germline array desilencing effect in *C. elegans*
- The desilencing response tracks with germline apoptosis and embryonic lethality
- Ancestrally exposed F3 germlines show a dramatic reduction in H3K9me3 and H3K27me3
- JMJD-2 and JMD-3/UTX-1 demethylases are required for BPA's transgenerational effects

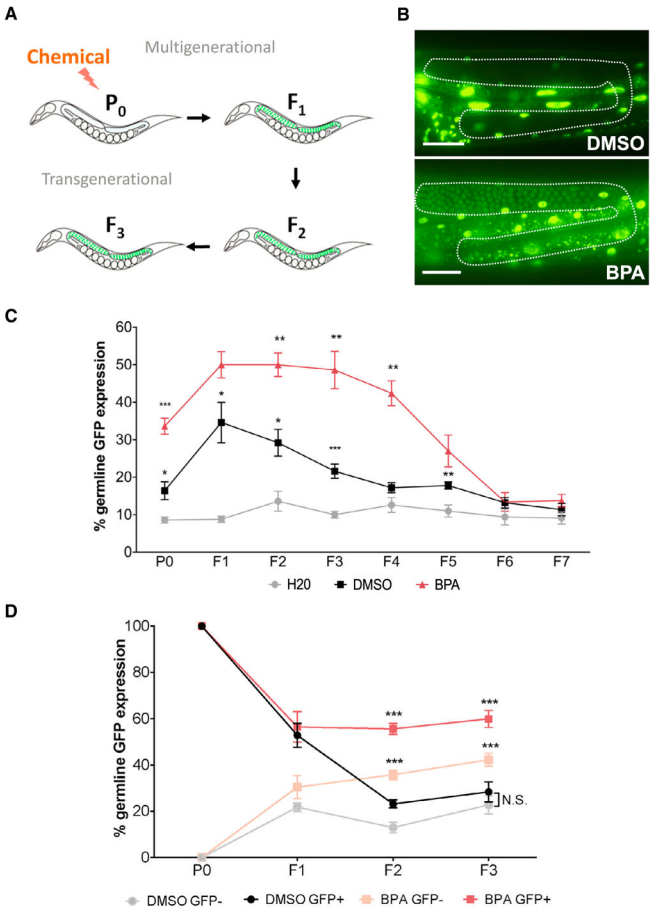

Figure 1. BPA Exposure Elicits a Transgenerational Desilencing of a Repetitive Array

(A) Exposure scheme. Nematodes are exposed to the chemicals of interest for 48 hr at the parental (P0) generation. Worms carrying the integrated array *pkIs1582* [*let-858*::GFP; *rol-6*(*su1006*)] express GFP in all somatic nuclei but silence the array in the germline. This strain is used to monitor the array desilencing over multiple generations.

(B) Representative example of silenced (top) and desilenced (bottom) *pkIs1582* array expression in F3 germlines (dashed lines). Scale bar, 50 μm.

(C) Percentage of worms displaying germline de-silencing (y axis) at each generation (x axis). n = 5–10, 30 worms each; *p ≤ 0.05, **p ≤ 0.01, and ***p ≤ 0.001. Significance is indicated for BPA versus DMSO above the BPA line and DMSO versus water above the DMSO line.

(D) Lineage analysis of the germline desilencing response. Worms were sorted following exposure at the P0 generation based on their germline GFP expression. Their progeny was then followed and examined for 3 additional generations. n = 5–10, 30 worms each; ***p ≤ 0.001. BPA is compared to DMSO within each GFP status category (e.g., BPA/GFP+ versus DMSO/GFP+). All data are represented as mean ± SEM.

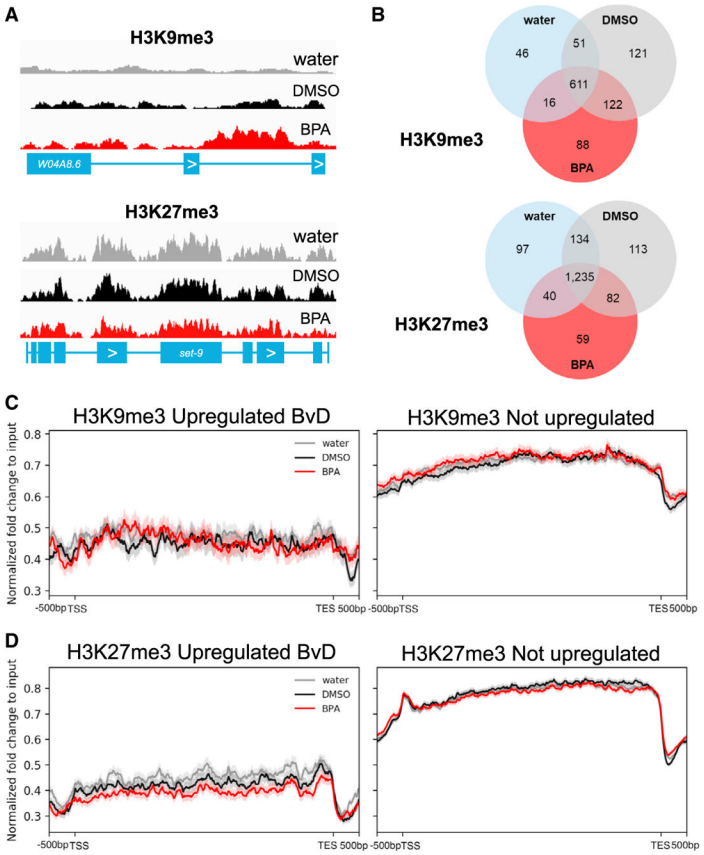

Figure 2. BPA-Induced Transgenerational Reduction in H3K9me3 and H3K27me3 Identified by ChIP-Seq

(A) Examples of ChIP-seq gene plots for H3K9me3 and H3K27me3 from F3 nematodes.

(B) Venn diagram from genes with peak calling in each of the treatment groups.

(C) Average H3K9me3 histone modification fold enrichment signals from gene bodies of either silenced upregulated genes (left panel) or silenced non-upregulated genes (right panel) after BPA treatment. Lightly shaded regions indicate the SE.

(D) Average H3K27me3 histone modification fold enrichment signals from gene bodies of either silenced upregulated genes (left panel) or silenced non-upregulated genes (right panel) after BPA treatment. Lightly shaded regions indicate the SE.

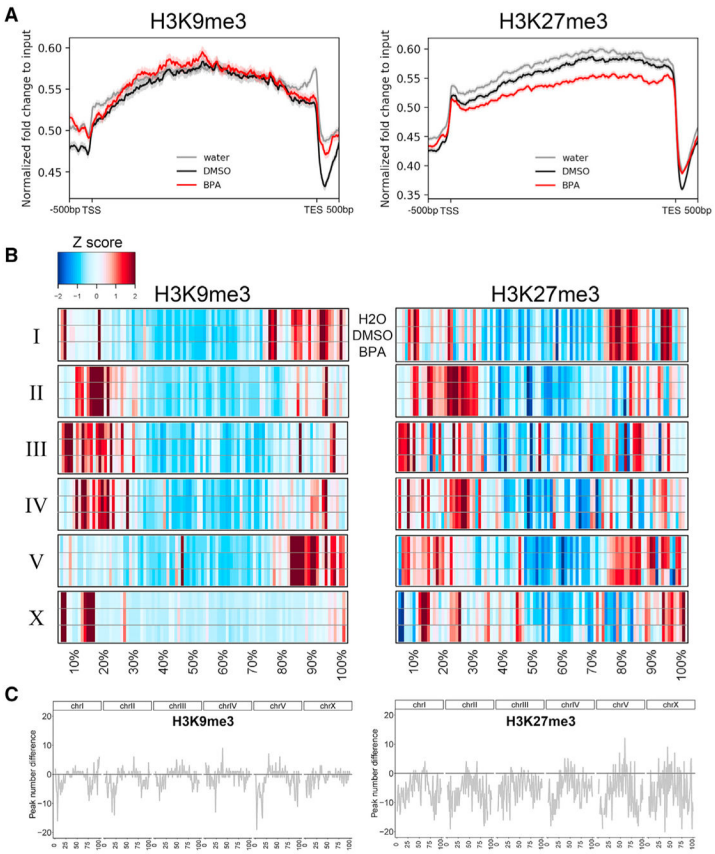

Figure 3. BPA Treatment Causes Transgenerational Intra-chromosomal Redistribution of Histone Modifications

(A) Average H3K9me3 (left) and H3K27me3 (right) histone modification fold enrichment signals from gene bodies of all genes. Shaded regions indicate SE.

(B) Heatmap of averaged H3K9me3 (left) and H3K27me3 (right) histone modification fold enrichment signals in 100 sub-regions across all chromosomes. *Z* scores were calculated on averaged values in each chromosome and sample.

(C) Difference in unique peak-calling numbers between BPA and DMSO from H3K9me3 (left) and H3K27me3 (right) along all chromosome sub-regions. The y axis indicates unique peak numbers calculated by BPA minus DMSO by region.

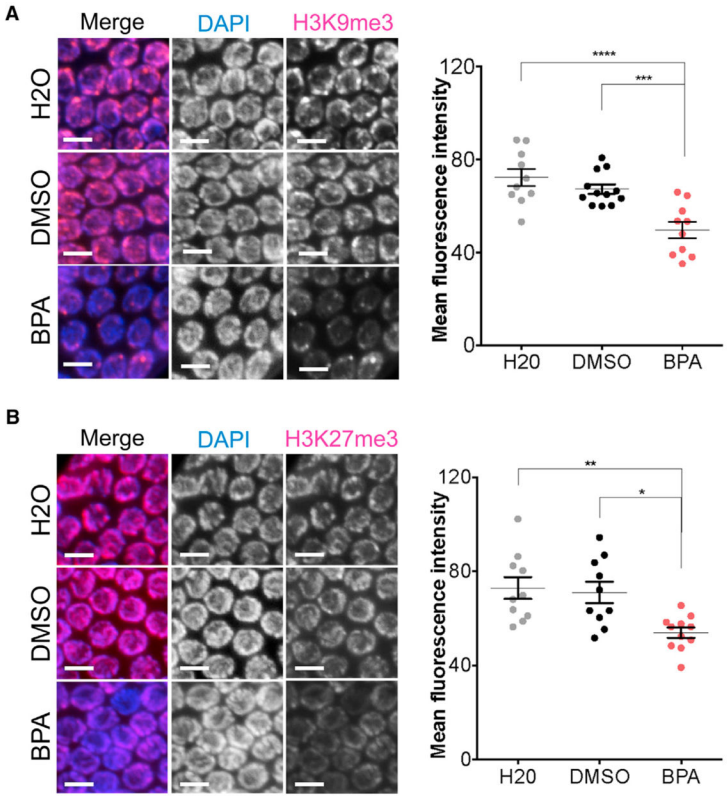

Figure 4. Ancestral BPA Exposure Decreases H3K9me3 and H3K27me3 Levels in F3 Germlines

(A and B) Immunofluorescence images of mid-to-late pachytene germline nuclei from F3 worms ancestrally exposed to DMSO or BPA and stained for H3K9me3 (A) or H3K27me3 (B). DAPI is represented in blue and the histone mark of interest in magenta in the merge. All images shown were selected representative images of the mean values obtained after quantification of all germline nuclei from that exposure group. The corresponding fluorescence intensity quantification is shown on the right panels. n = 11–12 worms, 10 nuclei per worm; *p ≤ 0.05, **p ≤ 0.01, ***p ≤ 0.001, and ****p ≤ 0.0001, one-way ANOVA with Sidak correction. Scale bar, 5 μm. All data are represented as mean ± SEM.

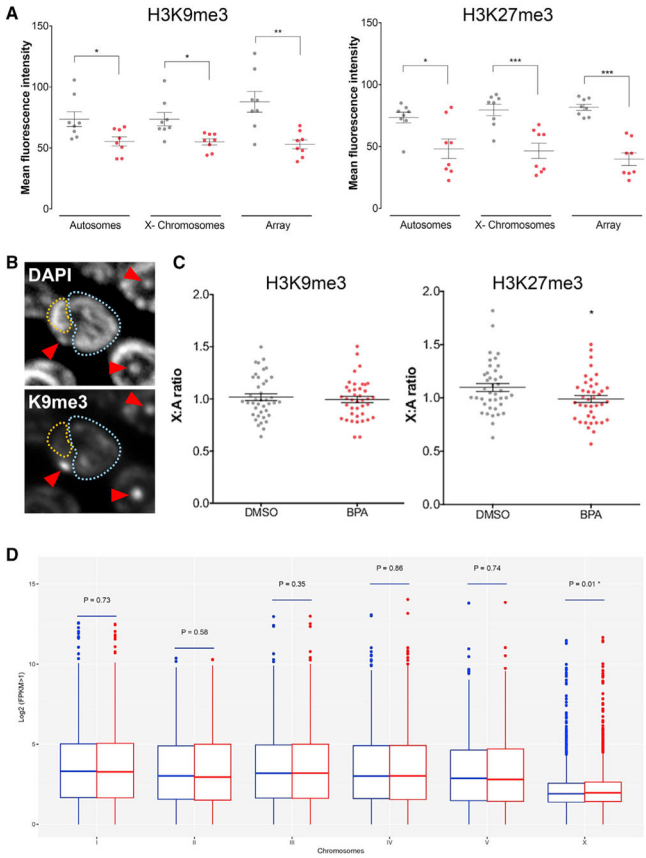

Figure 5. Ancestral BPA Exposure Leads to a Sharp Decrease in H3K9me3 and H3K27me3 on Autosomes, X Chromosomes, and an Extrachromosomal Array and an Up-regulation of X-Linked Genes

(A) Quantification of H3K9me3 and H3K27me3 levels on autosomes, X chromosomes, and an extrachromosomal array in the F3 generation following P0 exposure to either DMSO or BPA. Gray, DMSO; red, BPA. n = 8 worms, 5 nuclei per worm; *p ≤ 0.05, **p ≤ 0.01, and ***p ≤ 0.001.

(B) DAPI- (top) and H3K9me3- (bottom) stained nuclei. The colored dashed lines identify the auto-somes (blue) and the X chromosomes (orange). The red arrowheads identify the extrachromosomal array that is enriched in H3K9me3.

(C) Fluorescence intensity quantification of H3K9me3 and H3K27me3 levels is shown on the right. Gray is the X:A ratio for DMSO and red for BPA. n = 8 worms, 5 nuclei per worm; *p ≤ 0.05.

(D) Gene expression data from dissected F3 germlines showing all transcripts with FKPM > 1 following ancestral DMSO (blue) or BPA (red) exposure. X-linked genes show a modest but significant overall 2.36% increase in expression (p = 0.01). All data are represented as mean ± SEM.

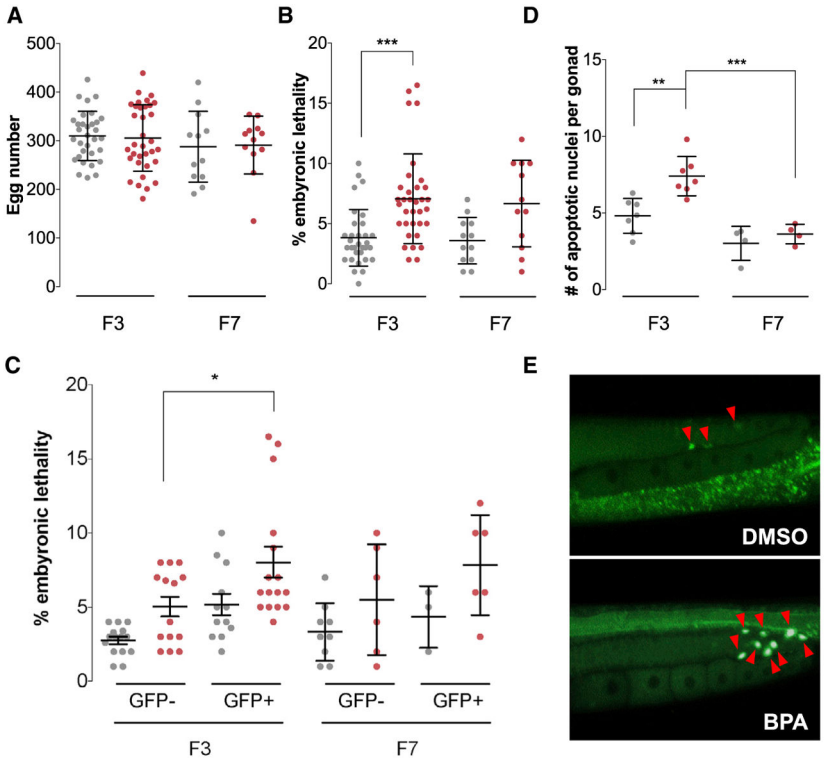

Figure 6. Transgenerational Impact of BPA on Fertility

(A) Number of eggs produced by F3 or F7 worms following P0 exposure to DMSO control (gray) or BPA (red).

(B) Percentage of lethality of embryos generated by F3 or F7 worms ancestrally exposed to either DMSO control or BPA. n = 23–33; ***p ≤ 0.001, two-way ANOVA.

(C) Embryonic lethality of F3 or F7 worms' progeny based on the GFP expression in the germline of F3 or F7 worms. n = 10; *p ≤ 0.05, two-way ANOVA.

(D) Number of apoptotic nuclei per gonadal arms of F3 or F7 worms. n = 7 repeats, 20 worms each; **p ≤ 0.01 and ***p ≤ 0.001, two-way ANOVA.

(E) Representative examples of acridine orange-stained F3 nematodes following P0 DMSO or BPA exposure. All data are represented as mean ± SEM.

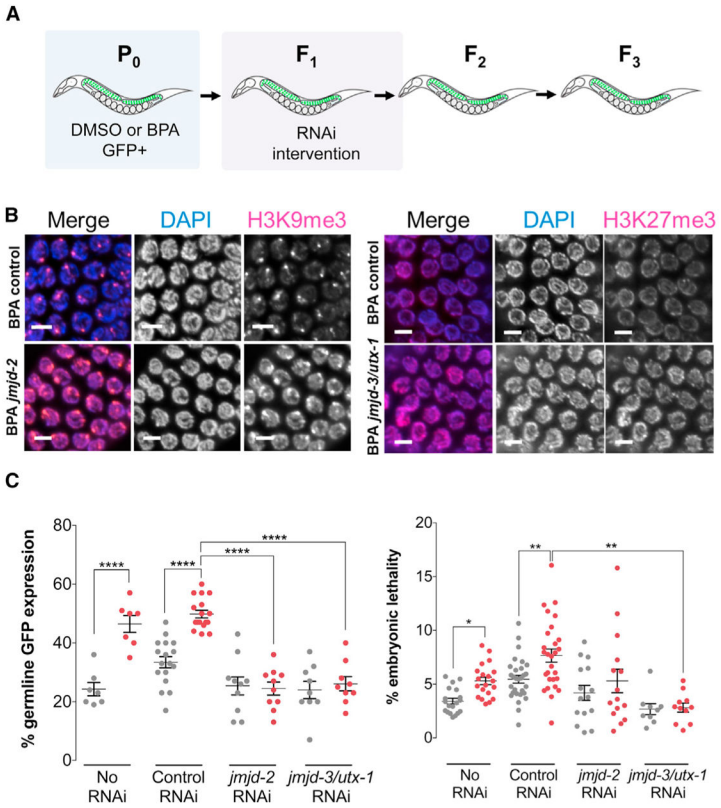

Figure 7. *jmjd-2* and *jmjd-3/utx-1* Demethylases Are Required for BPA-Induced Transgenerational Response

(A) Exposure and rescue experimental scheme. Following exposure to DMSO or BPA at the P0 generation, the progeny of GFP-positive P0 worms was collected and subjected to feeding RNAi until the F2. F3 worms were then collected and analyzed.

(B) Immunofluorescence images of mid-to-late pachytene germline nuclei from F3 worms ancestrally exposed to BPA and GFP-positive at the P0, stained for H3K9me3 or H3K27me3. DAPI is represented in blue and the histone mark of interest in magenta in the merge. All images shown were selected representative images of the mean values obtained after quantification of all germline nuclei from that exposure group (Figure S7A). Scale bar, 5 μm.

(C) RNAi rescue of ancestral DMSO- (gray) or BPA-(red) induced effects following either no F1 treatment, empty vector control, *jmjd-2*, or *jmjd-3/utx-1* feeding RNAi. n = 7–17 repeats, 30 worms each for desilencing assay and n = 4–8 repeats, 3–4 worms each for the embryonic lethality assay; *p ≤ 0.05, **p ≤ 0.01, and ****p ≤ 0.0001, two-way ANOVA. All data are represented as mean ± SEM.